Organometallic Derivatives of Orotic Acid. CO−Labilizing Ability of the Amido Group in Chromium and Tungsten Carbonyl Complexes

Donald J. Darensbourg,* Jennifer D. Draper, David L. Larkins, Brian J. Frost, and Joseph H. Reibenspies

Department of Chemistry, Texas A&M University, P.O. Box 300012, College Station, Texas 77842

Received March 4, 1998

Novel orotic acid and uracil derivatives of tungsten and chromium(0), $[Et_4N]_2[Cr(CO)_4(orotate)]$ (**1**), $[Et_4N]_2[W(CO)_4(orotate)]$ (**2**), $[Et_4N]_2[W(CO)_4(dihydroorotate)]$ (**3**), and $[Et_4N][W(CO)_5(uracilate)]$ (**4**) [where orotate = $(C_5H_2O_4N_2)^{2-}$; dihydroorotate = $(C_5H_4O_4N_2)^{2-}$; uracilate = $(C_4H_3O_2N_2)^-$], have been synthesized via reaction of $M(CO)_5THF$ with the tetraethylammonium salt of the corresponding acid or uracil. These complexes have been characterized in solution by IR and ^{13}C NMR spectroscopy and in the solid state by X-ray crystallography. The geometry of the metal dianions in **1** and **2** is that of a distorted octahedron consisting of four carbonyl ligands and a nearly planar five-membered orotate chelate ring, bound through the N1 and one of its carboxylate oxygen atoms. The uracil ring, including the exocyclic oxygens, itself deviates from planarity by only 0.009 Å. However, the structure of complex **3**, which closely resembles that of complexes **1** and **2**, has a puckered uracil ring. The structure of complex **4** consists of the uracilate ligand bound through the deprotonated N1 to a tungsten pentacarbonyl fragment. Although the orotate complexes are resistant to thermal decarboxylation, they readily undergo decarbonylation reactions. In this regard, quantitative investigations of the lability of the carbonyl ligands on complexes **1**−**4** have been carried out. All complexes exhibited a low energy barrier for CO dissociation as demonstrated by ^{13}CO exchange studies. For example, the first-order rate constants for intermolecular CO exchange in complexes **2** and **3** were measured to be 6.05×10^{-4} and 3.17×10^{-3} s^{-1} at 0 °C, respectively. This facile CO dissociation is attributed to competition of the metal center with the uracil ring for the π donation of electron density from the deprotonated N1 atom of the orotate ligand. As expected, this interaction is enhanced when the pseudoaromaticity of the uracil ring is disrupted in complex **3**. The activation parameters for the intermolecular exchange of CO in complex **2** were determined to be $\Delta H^{\ddagger} = 63.2 \pm 3.8$ kJ/mol and $\Delta S^{\ddagger} = -82.8 \pm 13.0$ J/mol·K, values consistent with a bond-making/bond-breaking (M···CO/M$\overset{\curvearrowleft}{-}$N) mechanistic pathway. The rate of intermolecular CO exchange was similarly examined in complex **4**. The uracilate ligand displayed a π donating capability comparable to that seen for chloride in the $W(CO)_5Cl^-$ anion but much less π donor character than the phenoxide ligand in $W(CO)_5OPh^-$. The activation parameters of the CO exchange process in complex **4** were found to be $\Delta H^{\ddagger} = 106.9 \pm 4.3$ kJ/mol and $\Delta S^{\ddagger} = 16.3 \pm 13.7$ J/mol·K.

Introduction

The superior capability of amido ligands to serve as π donating ligands in low-valent organometallic complexes has been substantially documented.[1] For example, Caulton has reported −NHPh to be a similar or better π donor ligand than −OPh in low-valent, sixteen-electron derivatives of ruthenium(II).[2] As a consequence of this property of amido ligands it is expected that they would serve as CO-labilizing groups in metal carbonyl derivatives. This phenomenon usually results from π stabilization of the transition-state and subsequently of the unsaturated intermediate arising from ligand dissociation, i.e., *intramolecular* RHN$\overset{\curvearrowleft}{-}$M π donation which leads to electronic saturation. Indeed, we have recently shown that the coordinatively and electronically unsaturated amido anionic derivatives of tungsten(0) carbonyl, $[W(CO)_3OC_6H_4NH]^{2-}$ and $[W(CO)_3NHC_6H_4NH]^{2-}$, are quite stable and even crystallographically characterizable as a consequence of the π donating ability of the amido ligands.[3]

In closely related studies we have attributed the greatly enhanced CO lability exhibited in selected amino acid derivatives of tungsten hexacarbonyl, e.g., $W(CO)_4(O_2CCH_2NH_2)^-$ and $W(CO)_4(O_2CCH_2NHMe)^-$, to the transient formation of a substitutionally labile amido intermediate.[4] This is reminiscent of the well-accepted SN_{1CB} mechanism for ligand substitution involving the $Co(NH_3)_5X^{2+}$ complex cation.[5] To further investigate this reaction process we have begun an examination of organometallic derivatives of orotic acid, an amino acid where N1 is generally deprotonated when it binds to a metal center.[6] The numbering scheme for orotic acid and the product of its decarboxylation, uracil, are shown below. Also provided is the structure of 5,6-dihydroorotic acid in which the pseudoaromaticity of the uracil ring is dissipated.

(1) Caulton, K. G. *New J. Chem.* **1994**, *18*, 25.
(2) Poulton, J. T.; Folting, K.; Streib, W. E.; Caulton, K. G. *Inorg. Chem.* **1992**, *31*, 3190.
(3) Darensbourg, D. J.; Klausmeyer, K. K.; Reibenspies, J. H. *Inorg. Chem.* **1996**, *35*, 1535.
(4) (a) Darensbourg, D. J.; Atnip, E. V.; Klausmeyer, K. K.; Reibenspies, J. H. *Inorg. Chem.* **1994**, *33*, 5230. (b) Darensbourg, D. J.; Draper, J. D.; Reibenspies, J. H. *Inorg. Chem.* **1997**, *36*, 3648.
(5) Tobe, M. L. *Adv. Inorg. Bioinorg. Mech.* **1983**, *2*, 1.
(6) (a) Mutikainen, I. *Ann. Acad. Sci. Fenn. Ser. A2, Chem.* **1988**, 217, and references therein. (b) Ruf, M.; Weis, K.; Vahrenkamp, H. *Inorg. Chem.* **1997**, *36*, 2130.

S0020-1669(98)00233-X CCC: $15.00
Published on Web 05/02/1998

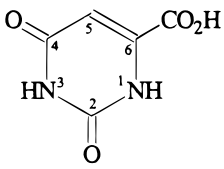

orotic acid

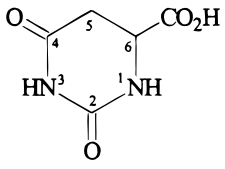

dihydroorotic acid

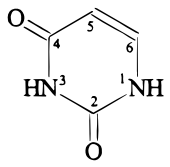

uracil

Orotic acid is important in pyrimidine biosynthesis, i.e., orotic acid is a precursor in the synthesis of the cytidine and thymidine nucleotides, and it has been confirmed that metal ions are necessary for this process.[7] Relevant to this, there is much current interest in the mechanistic aspects of the enzymatic decarboxylation reaction of orotidylic acid to uridine-5′-phosphate, the starting point for the synthesis of the cytidine and thymidine nucleotides.[8,9] The enzymatic catalyzed decarboxylation process displays a catalytic proficiency of 2.0×10^{23} M^{-1}, the most enhanced rate for a known enzymatic reaction. The nonenzymatic $t_{1/2}$ value at 25 °C of 78 million years was obtained from the decarboxylation of 1-methylorotic acid.[8] Lee and Houk have proposed on the basis of theoretical studies that the greatly accelerated enzymatically catalyzed process occurs by way of a resonance-stabilized carbene intermediate afforded subsequently to proton transfer at O4 from a lysine group of the enzyme.[9]

Furthermore, metal orotates are proposed as biological carriers for a variety of metal ions.[10] Hence, our interest in the bonding modes exhibited by orotate to low oxidation state metal species, coupled with the role of the amido ligand as a CO-labilizing group, has prompted us to investigate group 6 metal carbonyl derivatives of orotic acid. Specifically, the $[Et_4N]_2[M(CO)_4$-(orotate)] (M = Cr, W) derivatives have been synthesized and characterized both in solution and the solid-state, and the rates of CO dissociation have been determined via ^{13}CO exchange studies. When the heterocyclic N1 atom is deprotonated, its electron density is delocalized within the pseudoaromatic uracil ring and the exocyclic carbonyl oxygen atoms. Hence, there is expected to be competition of the ring system vs the unsaturated metal center upon M−CO dissociation for the electron density provided by the pseudoamido ligand. In turn, the effective competitiveness of the unsaturated metal center for this electron density is anticipated to be reflected in the rate constant for CO dissociation. This concept is further examined by measuring the rate of CO dissociation in the $W(CO)_4$(dihydroorotate)$^{2-}$ dianion.

For comparative purposes we have performed similar structural and reactivity studies on the $[W(CO)_5$(uracilate)$]^-$ anion, where the uracilate ligand is also bonded to the metal center via the deprotonated N1 atom. The $W(CO)_5$(uracilate)$^-$ anion is formally the product of decarboxylation of $W(CO)_4$(orotate)$^{2-}$ followed by subsequent protonation at C6 and addition of CO to the metal center. Although there are *no* metals involved in the enzyme system that catalyzes the decarboxylation of orotic acid, there are other decarboxylation processes which are catalyzed by metal complexes. Pertinent to this communication we have previously demonstrated that the $W(CO)_5(O_2CCH_2CN)^-$ anion serves as an effective catalyst precursor for the decarboxylation of cyanoacetic acid.[11]

Experimental Section

Methods and Materials. All manipulations were performed on a double manifold Schlenk vacuum line under an atmosphere of argon or in an argon-filled glovebox. Solvents were dried and deoxygenated by distillation from the appropriate reagent under a nitrogen atmosphere. Photolysis experiments were performed using a mercury arc 450 W UV immersion lamp purchased from Ace Glass Co. Infrared spectra were recorded on a Matteson 6022 spectrometer with DTGS and MCT detectors. Routine infrared spectra were collected using a 0.10-mm CaF_2 cell. ^{13}C NMR spectra were obtained on a Varian Unity XL-300 spectrometer. ^{13}CO was purchased from Cambridge Isotopes and used as received. $Cr(CO)_6$ and $W(CO)_6$ were purchased from Strem Chemicals, Inc., and used without further purification. Anhydrous orotic acid was obtained from Lancaster Synthesis, Inc., and used as received. Uracil, bis(triphenylphosphoranylidiene)ammonium chloride (PPNCl), and L-dihydroorotic acid were purchased from Aldrich Chemical and used without purification. Microanalyses were performed by Canadian Microanalytical Service, Ltd. (Delta, B C, Canada).

Synthesis of $[Et_4N]_2[C_5H_2N_2O_4]$ and $[Et_4N]_2[C_5H_4N_2O_4]$ Salts. The synthesis of these salts was accomplished by adding dropwise 2 equiv (2.8 mmol) of Et_4NOH, 25% in MeOH, to 1.4 mmol of anhydrous orotic acid or L-dihydroorotic acid stirring in MeOH, affording a cloudy solution. The mixture was stirred for 1 h, after which the MeOH was removed under vacuum overnight, leaving behind a white powder. Anal. Calcd for $[Et_4N]_2[C_5H_2N_2O_4]$, $C_{21}H_{42}N_4O_4$: C, 60.84; H, 10.21; N, 13.51. Found: C, 58.58; H, 10.21; N, 12.86.

Synthesis of $[Et_4N]_2[M(CO)_4$(orotate)], 1 and 2. The synthesis of $[Et_4N]_2[M(CO)_4(C_5H_2N_2O_4)]$ (where M = Cr or W and orotate = $C_5H_2N_2O_4^{2-}$) was accomplished in yields in excess of 85% by the reaction of 1.4 mmol of $M(CO)_5$THF (prepared by photolysis of 0.300 g of $Cr(CO)_6$ or 0.500 g of $W(CO)_6$ in THF for 1 h) with 1 equiv of the deprotonated orotic acid. The $M(CO)_5$THF intermediates are identified by their ν(CO) infrared spectra: M = Cr, 2073 (w), 1936 (s), 1894 (m); M = W, 2073 (w), 1929 (s), 1890 (m) cm^{-1}. Longer photolysis times for $W(CO)_6$ will lead to production of *cis*-$W(CO)_4$-$(THF)_2$, ν(CO): 2013 (w), 1876 (vs), 1830 (m) cm^{-1}. After 1 h, the THF was removed under vacuum, yielding a light orange (when M = W) or a dark orange (when M = Cr) powder. The powders were washed with hexanes to remove any residual $M(CO)_6$, dissolved in CH_3-CN and filtered through Celite. Crystals were obtained of the $[Et_4N]_2$ $[Cr(CO)_4$(orotate)] complex (**1**) by the slow diffusion of diethyl ether into a concentrated CH_3CN solution of the complex at −10 °C; crystals of complex **2**, $[Et_4N]_2$ $[W(CO)_4$(orotate)],were similarly obtained at room temperature. Anal. Calcd for $[Et_4N]_2[Cr(CO)_4(C_5H_2N_2O_4)]$ (**1**), $[C_{25}H_{42}N_4O_8Cr]$: C, 51.89; H, 7.32; N, 9.68. Found: C, 51.85; H, 7.73; N, 9.68. Anal. Calcd for $[Et_4N]_2[W(CO)_4(C_5H_2N_2O_4)]$ (**2**), $[C_{25}H_{42}N_4O_8W]$: C, 42.26; H, 5.96; N, 7.89. Found: C, 42.14; H, 6.16; N, 7.96.

Synthesis of $[Et_4N]_2[W(CO)_4$(L-dihydroorotate)], 3. The synthesis of $[Et_4N]_2[M(CO)_4(C_5H_4N_2O_4)]$ (where L-dihydroorotate = $C_5H_4N_2O_4^{2-}$) was accomplished in yields in excess of 85% by the reaction of 0.64 mmol of $M(CO)_5$THF (prepared by photolysis of 0.223 g of $W(CO)_6$ in THF for forty minutes) with one equivalent of the deprotonated L-dihydroorotic acid $[Et_4N]_2[C_5H_4N_2O_4]$. After 1 h, the THF was removed under vacuum, yielding a yellow powder. The powder was washed in hexanes to remove any residual $M(CO)_6$, dissolved in CH_3-

(7) Victor, J.; Greenberg, L. B.; Sloan, D. L. *J. Biol. Chem.* **1979**, *254*, 2647.
(8) (a) Radzicka, A.; Wolfenden, R. *Science* **1995**, *267*, 90. (b) Beak, P.; Siegel, B. *J. Am. Chem. Soc.* **1976**, *98*, 3601.
(9) Lee, J. K.; Houk, K. N. *Science* **1997**, *276*, 942.
(10) (a) Kumberger, O.; Reide, J.; Schmidbaur, H. *Chem. Ber.* **1991**, *124*, 2739. (b) Bach, I.; Kumberger, O.; Schmidbaur, H. *Chem. Ber.* **1990**, *123*, 2267.
(11) Darensbourg, D. J.; Chojnacki, J. A.; Atnip, E. V. *J. Am. Chem. Soc.* **1993**, *115*, 4675.

Table 1. Crystallographic Data for Complexes **1**−**4**

	1	**2**	**3**	**4**
empirical formula	$C_{28}H_{46.50}N_{5.50}O_8Cr$	$C_{28}H_{46.50}N_{5.50}O_8W$	$C_{27}H_{46}N_5O_{8.5}W$	$C_{45}H_{33}N_3O_5P_2W$
fw	640.21	772.06	759.53	973.58
space group	*C*2/*c*	*C*2/*c*	$P2_12_12_1$	$P\bar{1}$
V, Å^3	7004(2)	6961(2)	6653.4(11)	2064.3(7)
Z	8	8	8	2
d_{calc}, g/cm^3	1.214	1.473	1.517	1.566
a, Å	16.552(3)	16.383(2)	13.488(2)	10.173(2)
b, Å	12.122(2)	12.121(1)	13.7357(11)	13.973(3)
c, Å	34.929(7)	34.939(4)	35.913(3)	14.959(3)
α, deg	−	−	−	81.95(3)
β, deg	91.99(3)	90.121(10)	−	88.90(3)
γ, deg	−	−	−	78.67(3)
T, K	193	193	193	193
μ(Mo Kα), mm^{-1}	3.131	3.369	3.525	2.924
wavelength, Å	1.547 18	0.710 73	0.710 73	0.710 73
R_F,[a]%	7.95	6.65	5.35	7.66
R_{wF},[b]%	17.02	14.40	12.07	9.81

[a] $R_F = \sum|F_o - F_c|/\sum F_o$. [b] $R_{wF} = \{[\sum w(F_o^2 - F_c^2)^2]/(\sum wF_o^2)\}^{1/2}$.

CN and filtered through Celite. Crystals of the $[Et_4N]_2$ [$W(CO)_4$(L-dihydroorotate)] complex (**3**) were obtained by the slow diffusion of diethyl ether into a concentrated CH_3CN solution of the complex at room temperature. Anal. Calcd for $[Et_4N]_2[W(CO)_4(C_5H_4N_2O_4)]$ (**3**), $[C_{25}H_{44}N_4O_8W]$: C, 42.14; H, 6.22; N, 7.86. Found: C, 43.86; H, 6.85; N, 7.95.

Synthesis of [Et$_4$N][W(CO)$_5$(uracilate)], 4. The synthesis of [Et_4N]-[$W(CO)_5$(uracilate)] was accomplished in yields greater than 85% by reaction of 1.4 mmol of $W(CO)_5$THF (prepared by photolysis of 0.500 g of $W(CO)_6$ in 60 mL THF for 1 h), with 1.4 mmol of uracil, 1.4 mmol of NEt_4OH, and 10 mL of MeOH. The solvent was removed via vacuum after 1 h of stirring, leaving behind a yellow air-stable powder (0.697 g, 85%). The powder was recrystallized from a THF solution by layering with hexanes. The resulting powder was washed 2 × 20 mL hexanes and vacuum-dried, leaving an analytically pure yellow powder (0.612 g, 75%). Anal. Calcd for $[Et_4N][W(CO)_5(C_4H_3N_2O_2)]$ (**4**), $[C_{17}H_{23}O_7N_3W]$: C, 36.12; H, 4.10; N, 7.43; Found: C, 35.53; H, 4.29; N, 7.45. The PPN salt was synthesized in a manner similar to that of the NEt_4 salt, 1.4 mmol of $W(CO)_5$THF (prepared by photolysis of 0.500 g of $W(CO)_6$ in 60 mL of THF for 1 h) was reacted with 1.4 mmol of uracil and excess NaH. PPNCl (1.4 mmol) was then added to exchange the sodium cation for PPN^+. Crystals of the PPN^+ salt were obtained by layering a THF solution of $[PPN][W(CO)_5(C_4H_3N_2O_2)]$ with hexanes at ambient temperature.

X-ray Crystallography. [Et$_4$N]$_2$[M(CO)$_4$(orotate)] Derivatives (1 and 2). Crystal data and details of data collection are given in Table 1. A yellow-orange block of **1** and a yellow block of **2** were mounted on glass fibers with epoxy cement at room temperature and cooled in a liquid nitrogen cold stream. Preliminary examination and data collection were performed on a Rigaku AFC5R X-ray diffractometer (Cu Kα, λ = 1.541 78 Å radiation) for **1** and on a Siemens P4 X-ray diffractometer (Mo Kα, λ = 0.710 73 Å radiation) for **2**. Cell parameters were calculated from the least-squares fitting of the setting angles for 24 reflections. ω scans for several intense reflections indicated acceptable crystal quality. Data were collected for $4.0 \le 2\theta \le 50°$. Three control reflections, collected every 97 reflections, showed no significant trends. Background measurements by stationary-crystal and stationary-counter techniques were taken at the beginning and end of each scan for half the total scan time. Lorentz and polarization corrections were applied to 5297 for **1** and 6075 reflections for **2**. A semiempirical absorption correction was applied to **1** and **2**. A total of 5103 unique reflections for **1** and 5856 for **2**, with $|I| \ge 2.0\sigma(I)$, were used in further calculations. Both structures were solved by direct methods [Sheldrick, G. M. SHELXS Program Package; (1993)]. Full-matrix least-squares anisotropic refinement for all non-hydrogen atoms yielded and R = 0.0732, R_w = 0.1375 and S = 1.115 for **1** and R = 0.0603, R_w = 0.1253 and S = 1.147 for **2**. Hydrogen atoms were placed in idealized positions with isotropic thermal parameters fixed at 0.08. Neutral-atom scattering factors and anomalous scattering correction terms were taken from *International Tables for X-ray Crystallography*.

[Et$_4$N]$_2$[W(CO)$_4$(dihydroorotate)], 3. Crystal data and details of data collection are given in Table 1. An orange block of **3** was mounted on a glass fiber with epoxy cement at room temperature and cooled in a liquid nitrogen cold stream. Preliminary examination and data collection were performed on a Siemens P4 X-ray diffractometer (Mo Kα, λ = 0.710 73 Å radiation). Data collection methods and parameters are identical to that described for complexes **1** and **2**. Lorentz and polarization corrections were applied to 6131 reflections for **3**. A total of 6051 unique reflections were used in further calculations. Anisotropic refinement for all non-hydrogen atoms yielded R = 0.0535, R_w = 0.1207, and S = 1.010.

[PPN][W(CO)$_5$(uracilate)], 4. Crystal data and details of data collection are given in Table 1. A yellow block of **4** was mounted on a glass fiber with epoxy cement at room temperature and cooled in a liquid nitrogen cold stream. Preliminary examination and data collection were performed on a Siemens P4 X-ray diffractometer (Mo Kα, λ = 0.710 73 Å radiation). Data collection methods and parameters are identical to that described for complexes **1** and **2**. Lorentz and polarization corrections were applied to 6671 reflections for **4**. A total of 6667 unique reflections were used in further calculations. Anisotropic refinement for all non-hydrogen atoms yielded R = 0.0766, R_w = 0.1864, and S = 1.037.

Kinetic Measurements. The rates of ^{13}CO exchange in complexes **1**−**3** were determined by placing an acetonitrile solution of the corresponding complex (0.6 mmol in 20 mL) under an atmosphere of ^{13}CO. The kinetic data on complex **4** were obtained by placing an atmosphere of ^{13}CO over a THF solution of **4** (0.1 mmol in 30 mL of THF). The solutions were situated in a thermostated water bath at 0.0 °C for **1** and **3** and at a variety of temperatures for **2** (0.0, 5.0, 20.0, 25.0, 30.0, and 35.0 °C) and **4** (30.0, 40.1, 49.9, and 58.0 °C), and shaken periodically. Prior to obtaining a room-temperature IR of complexes **1**−**3**, the solutions were transferred via cannula to an evacuated test tube maintained at the appropriate temperature and the ^{13}CO atmosphere was removed by vacuum in order to quench the exchange process. In all complexes the exchange process was monitored by observing the decrease in absorbance of the highest frequency ν(CO) band of the starting complex as a function of time.

Results

Synthesis and Spectral and Structural Characterization. [Et$_4$N]$_2$[M(CO)$_4$(orotate)] (M = Cr, W), [Et$_4$N]$_2$[W(CO)$_4$-(dihydroorotate)], and [Et$_4$N][W(CO)$_5$(uracilate)]. The zero valent metal carbonyl derivatives of orotic acid, L-dihydroorotic acid and uracil were synthesized in greater than 85% yield by the labile ligand displacement reaction of $M(CO)_5$THF, obtained via photolysis of $Cr(CO)_6$ or $W(CO)_6$, with the doubly deprotonated tetraethylammonium salt of anhydrous orotic acid $[Et_4N]_2[C_5H_2N_2O_4]$ (**1**, **2**) or dihydroorotic acid $[Et_4N]_2$-

Table 2. Stretching Frequencies of the Carbonyl and Carboxylate Ligands in the $M(CO)_4(orotate)^{2-}$ (**1**, **2**), $M(co)_4(dihydroorotate)^{2-}$ (**3**), and $W(CO)_5(uracilate)^-$ (**4**) Anions[a]

complex[a]	ν(C≡O), cm^{-1}				ν(C=O), cm^{-1}		ν(C=O), cm^{-1}	
					asym	sym		
$[Cr(CO)_4(orotate)^{2-}]$	1990 (w)	1854 (vs)	1840 (sh)	1797 (m)[b]	1653	1362[c]	1641	1617[d]
$[W(CO)_4(orotate)^{2-}]$	1987 (w)	1842 (vs)	1829 (sh)	1792 (m)[b]	1659	1357[c]	1650	1643[d]
$[W(CO)_4(L\text{-dihydroorotate})^{2-}]$	1980 (w)	1838 (vs)	1830 (sh)	1782 (m)[b]	1647	1379[c]	1625[d,e]	–[e]
$[W(CO)_5(uracilate)^-]$	2065 (w)	1917 (vs)	1858 (m)[b]	–	–	–	1668	1639[d]

[a] As the tetraethylammonium salt. [b] Spectra determined in CH_3CN. [c] Carboxylate stretches. [d] Organic carbonyl stretches from the uracil ring. [e] One broad peak observed.

Scheme 1

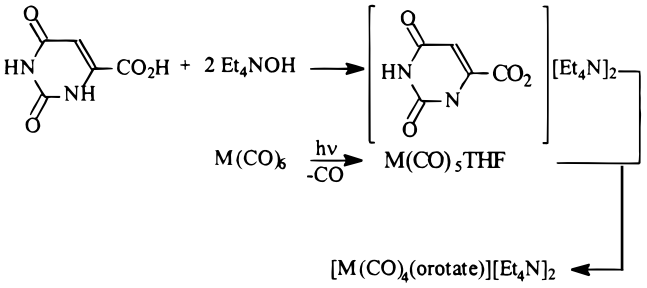

$[C_5H_4N_2O_4]$ (**3**), or the monodeprotonated PPN^+ or NEt_4^+ salts of uracil (**4**). Scheme 1 uses orotic acid to summarize the approach employed in the synthesis of complexes **1**−**3**. The reaction proceeds, as evident by the time-dependent ν(CO) infrared spectrum, by way of the displacement of THF by the carboxylic oxygen atom or the N1 nitrogen atom on the doubly deprotonated orotate ligand, followed shortly by the chelation to the metal center with concomitant loss of CO. Formation of either pentacarbonyl intermediate, i.e., metal−carboxylate[12] or metal-amide,[3] is anticipated to have labile CO ligands leading readily to a chelated product.

Complexes **1**−**3** exhibit a four-band pattern in the carbonyl region of the infrared spectrum consistent with a cis-disubstituted tetracarbonylmetal center, while complex **4** displays a three-band pattern typical of a monosubstituted pentacarbonyl derivative.[13] These frequencies, as well as those corresponding to the carboxylate stretches (**1**−**3**) and the organic carbonyls (ketones), are provided in Table 2. Because the CO ligands are such good probes of the electron-donating ability of the ancillary ligands in metal carbonyl derivatives, it is of interest to compare the ν(CO) values in the orotate complexes reported upon herein with the corresponding values for the glycine derivatives.[4] The average ν(CO) frequency in both the chromium and tungsten orotate complexes (**1** and **2**) is 11−12 cm^{-1} lower than those in the glycinate derivatives,[4] indicative of a significant enhancement of electron donating ability of the orotate dianion vs the glycinate monoanion. Presumably this greater donating ability of the orotate ligand is due to the presence of the additional negative charge provided by the amido group. Similarly, when the pseudoaromatic orotate ligand is replaced by the dihydroorotate ligand in the $W(CO)_4$ derivative, as expected the average ν(CO) frequency decreases by an additional 5 cm^{-1}. Likewise, the ν(CO) vibrations in the $W(CO)_5(uracilate)^-$ anion are on average shifted 13 cm^{-1} toward lower frequency than those observed for a typical saturated amine complex such as $W(CO)_5$(piperidine).[14,15]

Table 3 lists the ^{13}C NMR data for the complexes in both the CO and carboxylate regions of the spectra. As anticipated from the ν(CO) infrared data the ^{13}C NMR chemical shifts for the carbonyl ligands in the orotate derivatives are downfield of the corresponding values in the glycine complexes, further indication of a more electron-rich carbon center.[16] Chemical shift data for the $M(CO)_4$ moieties reveal a slight electronic difference between the CO ligand trans to oxygen versus the CO ligand trans to nitrogen. The ^{13}C NMR spectra of complexes **1**−**3** display three signals for the carbonyl carbons in an approximate 2:1:1 intensity ratio (see Figure 1). The more intense resonance for the two carbonyl ligands cis to both the nitrogen and oxygen atoms of the orotate or dihydroorotate ligands is observed upfield from the two smaller signals assigned

Table 3. ^{13}C NMR Data for the Carbonyl and Carboxylate Ligands in $M(CO)_4(orotate)^{2-}$ (**1**, **2**), $M(CO)_4(dihydroorotate)^{2-}$ (**3**), and $W(CO)_5(uracilate)^-$ (**4**) Anions

complex	^{13}C resonance, ppm		
	CO (axial)	CO (trans to N)	CO (trans to O)
$[Cr(CO)_4(orotate)^{2-}]$[a,b]	216.5	232.4	232.5[c]
$[W(CO)_4(orotate)^{2-}]$[a,b]	205.5	218.0	218.1[c]
$[W(CO)_4(L\text{-dihydroorotate})^{2-}]$[a,b]	207.4	218.7	219.6
$[W(CO)_5(uracilate)^-]$[a,d]	200.6	205.7	–

[a] Spectra determined in acetonitrile-d_3. [b] As the tetraethylammonium salt. [c] The assignments of the ^{13}C signals for CO groups trans to N vs those trans to O are based on the general observation that the ^{13}C resonance for a CO group trans to N is upfield relative to a CO group trans to O in $W(CO)_5$ derivatives (see e.g.: Todd, L. J.; Wilkinson, J. R. *J. Organomet. Chem.* **1974**, *77*, 1; Darensbourg, D. J.; Wiegreffe, H. P. *Inorg. Chem.* **1990**, *29*, 592). Nevertheless, the signals are quite close, and an absolute distinction is not needed at this time. [d] As the PPN salt.

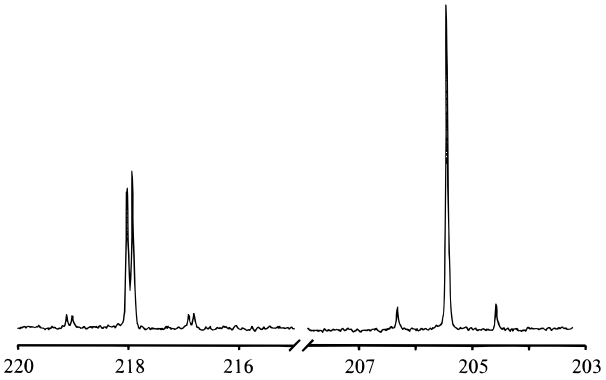

Figure 1. ^{13}C NMR spectrum of $[Et_4N]_2[W(CO)_4(orotate)]$ (**2**) in CD_3CN at 75 MHz.

(12) Darensbourg, D. J.; Joyce, J. A.; Bischoff, C. J.; Reibenspies, J. H. *Inorg. Chem.* **1991**, *30*, 1137.
(13) Braterman, P. S. *Metal Carbonyl Spectra*; Academic Press: New York, 1975.
(14) The three ν(CO) frequencies in $W(CO)_5$piperidine in acetonitrile solution appear at 2071 (w), 1926 (s), and 1882 (m) cm^{-1}. These are significantly shifted, in particular the vibrational mode trans to the amine, from the corresponding values determined in hexane solution.[15.]
(15) Dennenberg, R. J.; Darensbourg, D. J. *Inorg. Chem.* **1972**, *11*, 1.
(16) Mann, B. E.; Taylor, B. F. *^{13}C NMR Data for Organometallic Compounds*; Academic Press: New York, 1981.

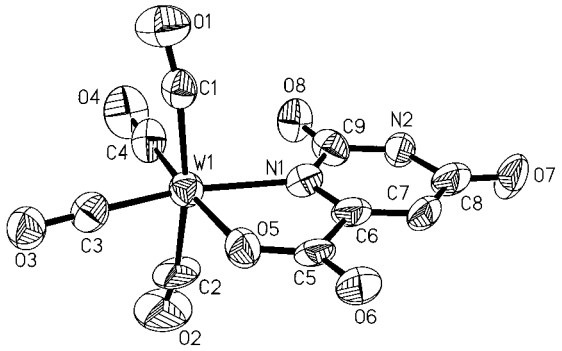

Figure 2. Thermal ellipsoid drawing of the anion of complex **2** with atomic numbering scheme.

Table 4. Selected Bond Lengths (Å) and Angles (deg) for $[Et_4N]_2[[W(co)_4(orotate)]$ (**2**)[a]

W(1)−C(1)	2.014(12)	O(8)−C(9)	1.253(14)
W(1)−C(2)	2.051(12)	N(1)−C(6)	1.347(14)
W(1)−C(3)	1.894(12)	N(1)−C(9)	1.39(2)
W(1)−C(4)	1.905(13)	N(2)−C(9)	1.387(14)
W(1)−O(5)	2.177(8)	N(2)−C(8)	1.39(2)
W(1)−N(1)	2.258(9)	C(5)−C(6)	1.55(2)
O(5)−C(5)	1.255(13)	C(6)−C(7)	1.35(2)
O(6)−C(5)	1.231(13)	C(7)−C(8)	1.42(2)
O(7)−C(8)	1.234(14)		
C(3)−W(1)−C(4)	90.5(5)	C(9)−N(2)−C(8)	127.5(11)
C(3)−W(1)−C(1)	89.1(4)	O(1)−C(1)−W(1)	167.0(10)
C(4)−W(1)−C(1)	82.9(5)	O(2)−C(2)−W(1)	169.4(13)
C(3)−W(1)−C(2)	86.9(5)	O(3)−C(3)−W(1)	178.3(10)
C(4)−W(1)−C(2)	84.0(5)	O(4)−C(4)−W(1)	178.6(9)
C(1)−W(1)−C(2)	166.2(5)	O(6)−C(5)−O(5)	128.3(11)
C(3)−W(1)−O(5)	93.7(4)	O(6)−C(5)−C(6)	117.4(10)
C(4)−W(1)−O(5)	175.6(4)	O(5)−C(5)−C(6)	114.3(10)
C(1)−W(1)−O(5)	96.1(4)	N(1)−C(6)−C(7)	125.3(11)
C(2)−W(1)−O(5)	97.3(5)	N(1)−C(6)−C(5)	114.0(9)
C(3)−W(1)−N(1)	165.9(4)	C(7)−C(6)−C(5)	120.7(11)
C(4)−W(1)−N(1)	103.6(4)	C(6)−C(7)−C(8)	120.5(11)
C(1)−W(1)−N(1)	93.4(4)	O(7)−C(8)−N(2)	119.4(12)
C(2)−W(1)−N(1)	93.7(5)	O(7)−C(8)−C(7)	128.2(12)
O(5)−W(1)−N(1)	72.2(3)	N(2)−C(8)−C(7)	112.4(11)
C(5)−O(5)−W(1)	123.0(7)	O(8)−C(9)−N(1)	123.3(10)
C(6)−N(1)−C(9)	118.1(10)	O(8)−C(9)−N(2)	120.5(11)
C(6)−N(1)−W(1)	116.5(7)	N(1)−C(9)−N(2)	116.2(12)
C(9)−N(1)−W(1)	125.3(8)		

[a] Estimated standard deviations are given in parentheses.

to the carbonyl ligands trans to the oxygen and nitrogen donors. Each resonance for complex **2** reveals satellites due to coupling with the ^{183}W nucleus (J_{C-W} = 132.9 Hz for axial carbonyls and an average of 111.1 Hz for the equatorial carbonyls). In complex 3 the axial carbonyl carbons couple to tungsten-183 with a constant of 125.7 Hz while the tungsten satellites for the peaks assigned to the equatorial carbons are weak and overlapping, making an accurate determination of J_{C-W} difficult. The ^{13}C NMR spectrum of **4** exhibits two signals for the carbonyl carbons in an approximate 4:1 ratio. The intense upfield peak (J_{W-C} = 130.1 Hz) is assigned to the four carbonyl ligands cis to the nitrogen atom of the uracilate ligand while the smaller downfield peak is attributed to the carbonyl ligand trans to the uracilate ligand.

The structures of complexes **1** and **2** were determined by crystallographic analysis; thermal ellipsoid drawings of the dianions are provided in Figures 1S and 2 and selected bond lengths and angles in Table 4. The unit cell also contains two tetraethylammonium counterions and an acetonitrile solvent molecule. The dianions of complexes **1** and **2** consist of an

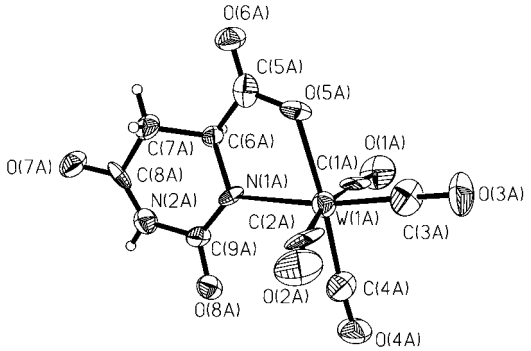

Figure 3. Thermal ellipsoid drawing of the anion of complex **3** with atomic numbering scheme.

orotate residue that forms a five-membered, almost planar,[17] chelate ring at the metal center through its deprotonated N1 atom and one of the carboxylate oxygen atoms. The slightly distorted octahedral geometry at the metal center is achieved by coordination of four carbonyl ligands. The metal centers in **1** and **2** deviate from the mean plane of the pyrimidine ring by only 0.030 and 0.004 Å, respectively. Furthermore, the pyrimidine rings, including the exocyclic oxygen atoms, do not exhibit large deviations from planarity (0.009 Å). This in turn is indicative of the N1 atom possessing essentially sp^2 hybridization. All intraligand distances in the pyrimidine ring lie within the range observed for a large variety of N1 coordinated uracils.[6]

The orotate ligand forms bite angles of 76.3(2) and 72.2(3)° with the metal atom in complexes **1** and **2**, respectively. The Cr−O bond length observed in **1** of 2.086(4) Å is significantly shorter than that noted in other amino acid derivatives of chromium(0); e.g., in $Cr(CO)_4(NH_2CH_2CO_2)^-$ the Cr−O bond length is 2.22(1) Å.[4b] On the other hand, the Cr−N bond distance (2.119(5) Å) in **1**, where nitrogen is deprotonated, is nearly identical to the Cr−N bond distance (2.15(1) Å) noted in the other amino acid derivative of chromium where the nitrogen is a neutral ligand. Unlike the chromium analogue, the W−O bond length in complex **2** of 2.177(8) Å is similar to that noted in other amino acid derivatives of tungsten(0); e.g., in $W(CO)_4(NH_2CH_2CO_2)^-$ the W−O bond length is 2.156(21) Å.[4a] However, the W−N bond distance (2.258(9) Å) in **2** when nitrogen is deprotonated is significantly shorter than the W−N bond distance (2.328(22) Å) in the glycine derivative.

The metal−carbonyl bond distances in complexes **1** and **2** exhibit similar trends. In each the average $M-C_{ax}$ bonds are longer than the average $M-C_{eq}$ bonds, i.e., 1.864(7) vs 1.800(7) Å for **1** and 2.03(1) vs 1.90(1) Å for **2**. The carboxylate and amide groups exhibit a small trans effect, giving equatorial Cr−C bond lengths of 1.777(6) (trans to nitrogen) and 1.822(8) Å (trans to oxygen) for **1** and W−C bond lengths of 1.89(1) (trans to nitrogen) and 1.91(1) Å (trans to oxygen) for **2**. The axial carbonyls ligands are somewhat bent, with M−C−O bond angles of 169.5(7) for **1** and 168.2(2) for **2**.

The structure of **3** determined by crystallographic analysis is presented in Figure 3. Selected bond lengths and angles are provided in Table 5. Although two molecules of the complex exist in the unit cell, both exhibit similar bond distances and bond angles. One molecule of water and one molecule of methanol are present in the unit cell in addition to the tetraethylammonium counterions. The dianion of complex **3** consists of an L-dihydroorotate residue bound in a five

(17) The mean plane defined by the CO_2 unit of the orotate ligand vs that defined by the atoms of the uracil fragment is tilted by only 1.5°.

Table 5. Bond Lengths (Å) and Angles (deg) for **3**[a]

W(1A)−C(3A)	1.92(2)	O(6A)−C(5A)	1.20(3)
W(1A)−C(2A)	1.97(2)	O(7A)−C(8A)	1.26(2)
W(1A)−C(4A)	1.97(2)	O(8A)−C(9A)	1.22(2)
W(1A)−C(1A)	2.00(2)	N(1A)−C(9A)	1.31(2)
W(1A)−O(5A)	2.211(12)	N(1A)−C(6A)	1.47(2)
W(1A)−N(1A)	2.231(13)	N(2A)−C(8A)	1.27(3)
O(1A)−C(1A)	1.16(3)	N(2A)−C(9A)	1.43(2)
O(2A)−C(2A)	1.20(3)	C(5A)−C(6A)	1.51(3)
O(3A)−C(3A)	1.21(2)	C(6A)−C(7A)	1.53(3)
O(4A)−C(4A)	1.13(2)	C(7A)−C(8A)	1.54(2)
O(5A)−C(5A)	1.32(2)		

C(3A)−W(1A)−C(2A)	85.2(11)	C(8A)−N(2A)−C(9A)	127(2)
C(3A)−W(1A)−C(4A)	87.8(9)	O(1A)−C(1A)−W(1A)	172(2)
C(2A)−W(1A)−C(4A)	84.6(9)	O(2A)−C(2A)−W(1A)	171(2)
C(3A)−W(1A)−C(1A)	85.9(11)	O(3A)−C(3A)−W(1A)	179(2)
C(2A)−W(1A)−C(1A)	168.2(10)	O(4A)−C(4A)−W(1A)	175(2)
C(4A)−W(1A)−C(1A)	87.3(9)	O(6A)−C(5A)−O(5A)	123(2)
C(3A)−W(1A)−O(5A)	97.0(8)	O(6A)−C(5A)−C(6A)	122(2)
C(2A)−W(1A)−O(5A)	95.2(7)	O(5A)−C(5A)−C(6A)	115(2)
C(4A)−W(1A)−O(5A)	175.2(7)	N(1A)−C(6A)−C(5A)	112(2)
C(1A)−W(1A)−O(5A)	93.5(6)	N(1A)−C(6A)−C(7A)	113(2)
C(3A)−W(1A)−N(1A)	169.9(8)	C(5A)−C(6A)−C(7A)	110(2)
C(2A)−W(1A)−N(1A)	94.9(9)	C(6A)−C(7A)−C(8A)	108(2)
C(4A)−W(1A)−N(1A)	102.3(7)	O(7A)−C(8A)−N(2A)	127(2)
C(1A)−W(1A)−N(1A)	95.3(8)	O(7A)−C(8A)−C(7A)	116(2)
O(5A)−W(1A)−N(1A)	73.0(5)	N(2A)−C(8A)−C(7A)	117(2)
C(5A)−O(5A)−W(1A)	121.0(12)	O(8A)−C(9A)−N(1A)	127(2)
C(9A)−N(1A)−C(6A)	117.5(14)	O(8A)−C(9A)−N(2A)	115(2)
C(9A)−N(1A)−W(1A)	127.4(11)	N(1A)−C(9A)−N(2A)	118(2)
C(6A)−N(1A)−W(1A)	114.0(11)		

[a] Estimated standard deviations are given in parentheses.

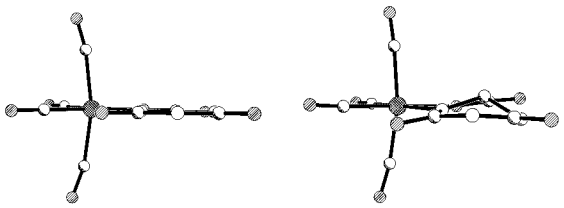

Figure 4. Ball and stick representation of complexes **2** and **3** comparing the planar orotate ring vs the puckered L-dihydroorotate ring.

membered chelate ring at the metal center. This is similar to the structures observed for complexes **1** and **2**; however, complex **3** differs from the orotate complexes in that the pyrimidine ring is no longer planar. This is readily observed in Figure 4 where the L-dihydroorotate complex (**3**) and the orotate complex (**2**) are shown from a side-on view with the uracil ring perpendicular to the plane of the page. The metal lies out of the chelate plane by 0.102 Å, and the pyrimidine ring itself deviates from planarity by 0.155 Å. Hence, in this instance the N1 atom of the heterocyclic ring exhibits more of an sp^3 type hybridization as compared with that in complex **3**.[18] The intraligand distances in the pyrimidine ring are similar to those found in the uracil ring with the exception of the C(6)−C(7) bond length. That is, an expected the bond distance lengthens from 1.31 Å in the orotate complex **2** to 1.53 Å in the dihydroorotate analogue, complex **3**.[19]

(18) A reviewer has suggested alternatively that the N1 atom could have sp^2 hybridization with a pure p orbital imperfectly aligned for donation to the metal center.

(19) The methyl ester of dihydroorotic acid exhibits a C(6)−C(7) bond length of 1.520 Å; see: Hambley, T. W.; Phillips, L.; Poiner, A. C.; Christopherson, R. I. *Acta Crystallogr., Sect. B (Struct. Sci.)* **1993**, *49*, 130.

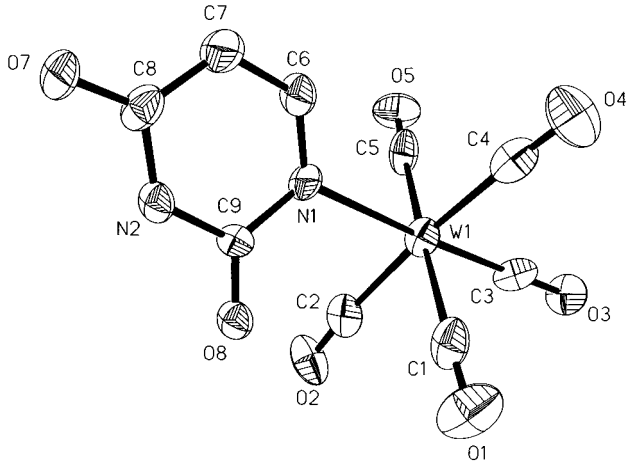

Figure 5. Thermal ellipsoid drawing of the anion of complex **4** with atomic numbering scheme.

Table 6. Bond Lengths (Å) and Angles (deg) for **4**[a]

W(1)−C(1)	2.07(2)	O(5)−C(5)	1.14(2)
W(1)−C(2)	2.04(2)	O(7)−C(8)	1.247(14)
W(1)−C(3)	1.960(12)	O(8)−C(9)	1.215(14)
W(1)−C(4)	2.03(2)	N(1)−C(6)	1.33(2)
W(1)−C(5)	2.026(13)	N(1)−C(9)	1.38(2)
W(1)−N(1)	2.281(8)	N(2)−C(8)	1.36(2)
O(1)−C(1)	1.14(2)	N(2)−C(9)	1.399(14)
O(2)−C(2)	1.15(2)	C(6)−C(7)	1.37(2)
O(3)−C(3)	1.171(14)	C(7)−C(8)	1.42(2)
O(4)−C(4)	1.15(2)		

C(1)−W(1)−N(1)	95.2(4)	C(6)−N(1)−C(9)	119.4(9)
C(2)−W(1)−N(1)	92.4(4)	C(6)−N(1)−W(1)	122.5(8)
C(3)−W(1)−N(1)	177.2(5)	C(9)−N(1)−W(1)	118.0(7)
C(4)−W(1)−N(1)	90.9(4)	C(8)−N(2)−C(9)	126.7(11)
C(3)−W(1)−C(5)	87.1(5)	O(1)−C(1)−W(1)	172.2(12)
C(3)−W(1)−C(4)	87.3(5)	O(2)−C(2)−W(1)	174.3(10)
C(5)−W(1)−C(4)	91.6(5)	O(3)−C(3)−W(1)	178.8(10)
C(3)−W(1)−C(2)	89.6(5)	O(4)−C(4)−W(1)	176.9(11)
C(5)−W(1)−C(2)	92.2(5)	O(5)−C(5)−W(1)	176.1(11)
C(4)−W(1)−C(2)	174.9(5)	O(7)−C(8)−N(2)	121.0(12)
C(3)−W(1)−C(1)	86.9(5)	O(8)−C(9)−N(2)	119.3(10)
C(5)−W(1)−C(1)	173.2(5)	N(1)−C(6)−C(7)	125.0(12)
C(4)−W(1)−C(1)	91.2(6)	N(1)−C(9)−N(2)	115.6(11)
C(2)−W(1)−C(1)	84.7(6)	C(6)−C(7)−C(8)	118.7(13)
C(5)−W(1)−N(1)	90.9(4)		

[a] Estimated standard deviations are given in parentheses.

The dihydroorotate residue in complex **3** forms a bite angle of 73.0(5)° with the metal center. The W−O bond length of 2.211(12) Å is longer than W−O bond length observed for either the tungsten orotate or glycinate derivatives. The observed W−N bond distance in complex **3** is 2.231(13) Å. While this is significantly shorter than that of the glycine derivative, it is similar to that observed in the orotate derivative where N1 is also deprotonated. The metal−carbonyl bond distances in complex **3** show the same general characteristics as those observed in complexes **1** and **2**. The average $M-C_{eq}$ bonds are slightly shorter than the average $M-C_{ax}$ bonds (1.985(2) Å vs 1.945(2) Å), and the axial carbonyl ligands are only slightly bent with M−C−O bond angles of 171(2) and 172(2)°.

The structure of **4** determined by crystallographic analysis is presented in Figure 5. Selected bond lengths and angles are provided in Table 6. Complex **4** consists of a uracilate ligand bound to a tungsten pentacarbonyl fragment through the deprotonated N1 atom with a W−N bond length of 2.281(8) Å. This bond distance is slightly shorter than the W−N bond length of 2.331(5) Å observed in $W(CO)_5$piperidine,[20] and

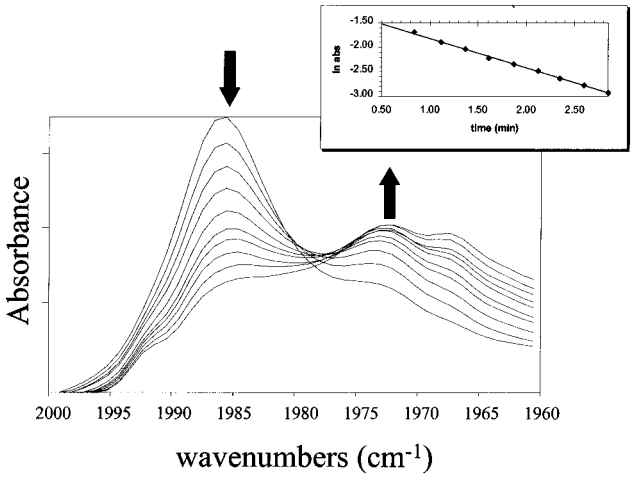

Figure 6. Spectral changes recorded for the process involving carbonyl ligand substitution in **2** with ^{13}CO at 30 °C. (Inset) Plot of ln(abs) vs time (min) for this process, indicating first-order kinetics.

slightly longer than the analogous parameter found in $W(CO)_5$pyridine of 2.26(1) Å.[21] The W−C bond length of the carbonyl ligand trans to the N1 is shorter (1.96(1) Å) than those cis to N1, with an average bond length of 2.04(2) Å. As observed in the orotate derivatives, the metal center in complex **4** is only out of the mean plane (0.012 Å) defined by the pyrimidine ring by 0.008 Å.

Carbon Monoxide Ligand Exchange Reactions. The reactivity of complexes **1**−**4** toward *dissociative* ligand exchange (e.g., as illustrated in eq 1 for the orotate derivatives) was investigated using ^{13}C-labeled carbon monoxide as an incoming ligand (L). It has been previously well established that these ligand substitution processes involving the weak nucleophile carbon monoxide as an incoming ligand are dissociative in nature.[4] Furthermore, the reaction was demonstrated by high-pressure NMR experiments not to involve chelate ring opening with concomitant formation of a pentacarbonyl transient that subsequently undergoes carbon monoxide loss.[4]

$$M(CO)_4(\text{orotate})^{2-} + {}^{13}CO \xrightarrow[n=1-4]{} M(CO)_{4-n}({}^{13}CO)_n(\text{orotate})^{2-} + n^{12}CO \quad (1)$$

The ligand substitution reactions were carried out in an excess of ^{13}C-labeled CO and were followed by infrared spectroscopy in the ν(CO) region. Specifically, the decrease in the absorbance of the high-frequency, well-isolated, CO stretching vibration in each respective complex was employed in monitoring the reactions' progress. Figure 6 depicts such spectral changes recorded for the process involving carbonyl ligand substitution in the $W(CO)_4(\text{orotate})^{2-}$ anion with ^{13}CO, whereas the inset in Figure 6 shows the decay of the parent dianion follows first-order kinetics. Disappearance of the all ^{12}CO species is indicated in Figure 6 with initial appearance of the mono-^{13}CO substituted shown. Over an extended period of time all the ^{13}-CO-substituted derivatives are observed. Similar kinetic data were noted for the other complexes investigated.

The initial site of CO incorporation into the $W(CO)_4(\text{orotate})^{2-}$ dianion was examined by ^{13}C NMR spectroscopy. When an atmosphere of ^{13}CO was placed over a CD_3CN solution of complex **2** in an NMR tube at −15 °C and the CO exchange process monitored (Figure 7), the first ^{13}C resonance to appear corresponds to the two axial CO ligands cis to both N and O atoms (205 ppm). The ^{13}C resonance due to the carbonyl ligand trans to oxygen (cis to the pseudoamido ligand) appears next, followed by the CO group trans to nitrogen. Hence, the enhanced rate and stereoselectivity of CO exchange is consistent with that expected for amido ligands being better cis-labilizing ligands than carboxylates.

Table 7. First−Order Rate Constants for CO Dissociation in Orotate and Dihydroorotate Metal Derivatives[a,b]

complex	temp (°C)	k (s^{-1}) × 10^4
1	0	49.0
2	0	6.05
	5	9.11
	25	54.2
	30	100
	35	133
3	0	31.7
$W(CO)_4$(glycinate)$^-$	0	0.225

[a] In CH_3CN. [b] All kinetic data were determined as the Et_4N^+ salts of the dianions to avoid significant ion-pairing effects (Payne, M. W.; Leussing, D. L.; Shore, S. G. *Organometallics* **1991**, *10*, 574).

The first-order rate constants for CO dissociation in complexes **1**−**3** including temperature-dependent data for complex **2**, are indicated in Table 7. For comparative purposes analogous kinetic data are provided for the $W(CO)_4$(glycinate)$^-$ anion.[4b] The following conclusions are readily apparent from the kinetic data in Table 7. In all of these anionic metal carbonyl derivatives there is a low barrier to CO dissociation, i.e., all the processes are very fast. For example, the rate constant for CO dissociation in $W(CO)_6$ has been extrapolated to have a value of 1.0×10^{-14} s^{-1} at 30 °C,[22] which is some 10^{-12} times smaller than the analogous value in complex **2**. As expected based on weaker metal−CO bonding, dissociation of the CO ligand in the $Cr(CO)_4(\text{orotate})^{2-}$ derivative is faster than that noted in the tungsten analogue.

Another revealing trend is the observation that CO dissociation in $W(CO)_4$(glycinate)$^-$ is slower by an order of magnitude than in $W(CO)_4(\text{orotate})^{2-}$, which in turn is significantly slower than CO dissociation in $W(CO)_4(\text{dihydroorotate})^{2-}$. This is best seen upon comparing the data in Table 7 at 0 °C. That is, as anticipated, the pseudoamido group in **2** is more CO-labilizing due to π donation to the metal center upon CO dissociation as compared with the glycinate derivative where there is only a transient formation of an amido intermediate. Furthermore, as the aromaticity in the heterocyclic ring is interrupted as in complex **3** the amido group becomes a better π donor and hence a better cis CO-labilizing ligand.[23,24] Nevertheless, the CO-labilizing abilities of the "amido" groups in complexes **2** and **3** are much less than what is seen for an amido group which is not stabilized via a neighboring carbonyl functionality. For instance, the amido ligands in the anionic complexes, $W(CO)_3[NHC_6H_4NH]^{2-}$ and $W(CO)_3[NHC_6H_4O]^{2-}$, are able to stabilize coordination and electronic unsaturation at the metal center. Consistent with a mechanistic pathway which involves both bond-breaking and bond-making, *i.e., M−C bond-breaking and M−N bond-making*, the activation parameters for intermolecular CO exchange in complex **2** were determined to be $\Delta H^{\ddagger} = 63.2 \pm 3.8$ kJ/mol and $\Delta S^{\ddagger} = -82.8 \pm 13.0$ J/mol·K.

(20) Moralejo, C.; Langford, C. H.; Bird, P. H. *Can. J. Chem.* **1991**, *69*, 2033.
(21) (a) Klement, U. *Z. Kristallogr.* **1993**, *208*, 111. (b) Tutt, L.; Zink, J. I. *J. Am. Chem. Soc.* **1986**, *108*, 5830.
(22) (a) Angelici, R. J. *Organomet. Chem. Rev.* **1968**, *3*, 173. (b) Darensbourg, D. J. *Adv. Organomet. Chem.* **1982**, *21*, 113.
(23) Lichtenberger, D. L.; Brown, T. L. *J. Am. Chem. Soc.* **1978**, *100*, 366.
(24) Davy, R. D.; Hall, M. B. *Inorg. Chem.* **1989**, *28*, 3524.

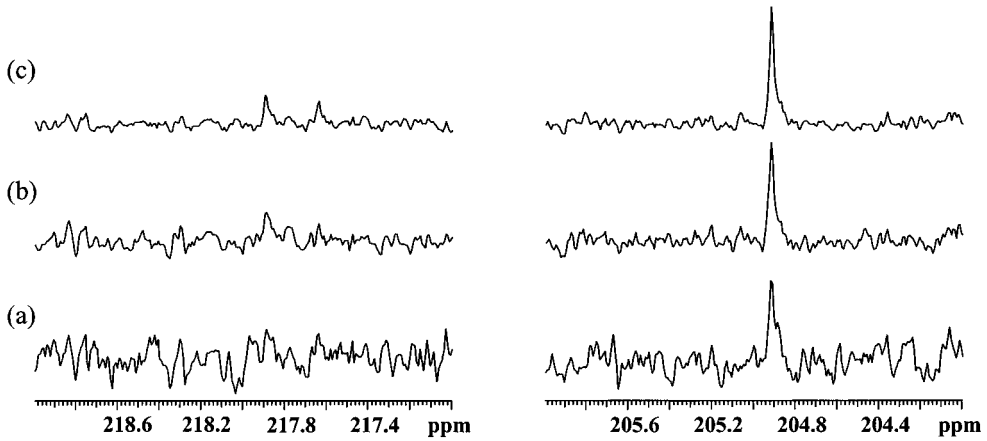

Figure 7. ^{13}C NMR of ^{13}CO exchange in complex **2** at −15 °C, (a) 13 min, (b) 22 min, and (c) 40 min after addition of ^{13}CO.

Table 8. Observed First-Order Rate Constants for the ^{13}CO Exchange of $[NEt_4][W(CO)_5(uracilate)]$ as a Function of Temperature[a]

temperature (°C)	k_{obs} (s^{-1}) × 10^4
30.0	0.183
40.1	0.617
49.9	2.667
58.0	6.850

[a] In THF.

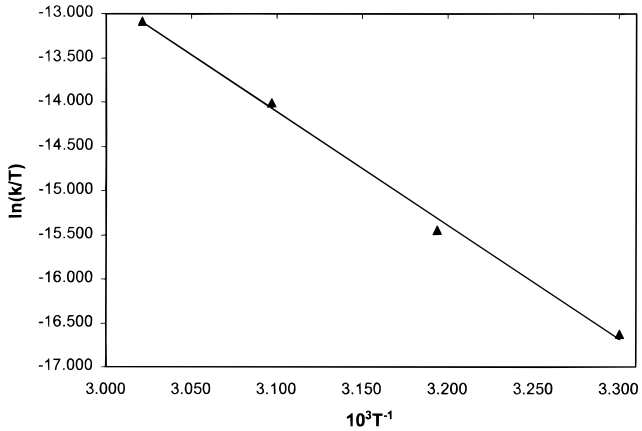

Figure 8. Eyring plot for intermolecular CO exchange in complex **4,** $[Et_4N][W(CO)_5(C_4H_3N_2O_2)]$.

In addition, the weak but quite significant π donating ability of the uracilate ligand is reflected in the kinetic parameters for the dissociation of CO in the complex $[Et_4N][W(CO)_5$(uracilate)]. Table 8 contains the temperature-dependent first-order rate constants for CO loss determined by the ^{13}CO-exchange process. The reaction as defined in eq 2 was monitored by the disappearance for the high-frequency ν(CO) band observed at 2061.8 cm^{-1} in THF. The Eyring plot, Figure 8, provided activation parameters $\Delta H^{\ddagger} = 106.9 \pm 4.3$ kJ/mol and $\Delta S^{\ddagger} = 16.3 \pm 13.7$ J/mol·K for the CO exchange process of complex **4**. The activation parameters and rates of CO

$$W(CO)_5(\text{uracilate})^- + {}^{13}CO \rightarrow W(CO)_{5-n}({}^{13}CO)_n(\text{uracilate})^- + {}^{12}CO \quad (2)$$

exchange for complex **4** can be compared to that of other cis-labilizing ligands such as phenoxides and chloride.[17] For example, the CO exchange rate for **4** is much slower than that for $W(CO)_5(OPh)^-$ ($k = 2.15 \times 10^{-2}$ s^{-1} at 5 °C),[25] just slightly slower than that for $W(CO)_5Cl^-$ ($k = 1.01 \times 10^{-4}$ s^{-1} at 5 °C),[25] and much faster than the CO exchange which occurs in the parent hexacarbonyl.[22] The corresponding enthalpies of activation ($\Delta H^{\ddagger}$) for CO dissociation vary accordingly with −OPh < uracilate < CO, specifically with values of 82.4 < 106.9 < 166 kJ/mol. Equation 2 should be distinguished from reactions involving group 6 pentacarbonyl complexes containing amine ligands. In these instances, the complexes undergo dissociative amine loss rather than facile CO exchange. To cite an example, $W(CO)_5$piperidine under an atmosphere of CO dissociates the amine ligand with a first-order rate constant of 1.30×10^{-5} s^{-1} at 60.3 °C yielding $W(CO)_6$ with no CO exchange occurring.[26]

Summary and Conclusions

Thermally stable orotic acid derivatives of chromium and tungsten carbonyls were prepared in good yield from the reactions of the $M(CO)_5$THF adducts with the tetraethylammonium salts of the corresponding acid.[27] The X-ray structures of the orotate derivatives of both metals revealed a distorted octahedral geometry about the metal centers which were associated with four carbonyl ligands and a *planar* orotate ring. The orotate ligand was bound to the metal center through the deprotonated nitrogen (1) atom and one of the carboxylate oxygen atoms. ^{13}C NMR and ν(CO) infrared spectroscopies indicated the orotate dianion to possess significantly enhanced electron donating ability as compared with the glycinate monoanion similarly bound to $M(CO)_4$ fragments. Furthermore, the dihydroorotate dianion exhibited an even greater electron donating ability toward the metal tetracarbonyl moiety. Although the orotate metal carbonyl derivatives exhibited *no* tendency to undergo thermal *decarboxylation* in solution at 50 °C, these complexes readily underwent *decarbonylation* at temperatures as low as 0 °C. That is, carbon monoxide ligand exchange reactions carried out in the presence of the ^{13}CO demonstrated the orotate metal carbonyl complexes to contain very labile CO ligands, with first-order rate constants for CO

(25) (a) Darensbourg, D. J.; Klausmeyer, K. K.; Reibenspies, J. H. *Inorg. Chem.* **1995**, *34*, 1933. (b) Darensbourg, D. J.; Klausmeyer, K. K.; Draper, J. D.; Chojnacki, J. A.; Reibenspies, J. H. *Inorg. Chim. Acta* **1998**, *270*, 405.
(26) Darensbourg, D. J.; Ewen, J. A. *Inorg. Chem.* **1981**, *20*, 4168.
(27) There are a limited number of organometallic derivatives of amino acids currently in the literature. For additional contributions by others, see: (a) Meder, H.-J.; Beck, W. *Z. Naturforsch.* **1986**, *41B*, 1247. (b) Petri, W.; Beck, W. *Chem. Ber.* **1984**, *117*, 3265. (c) Grotjahn, D. B.; Groy, T. L. *J. Am. Chem. Soc.* **1994**, *116*, 6969. (d) Schubert, U.; Tewinkel, S.; Möller, F. *Inorg. Chem.* **1995**, *34*, 995. (e) Severin, K.; Mihan, S.; Beck, W. *Chem. Ber.* **1995**, *128*, 1127. (f) Grotjahn, D. B.; Joubran, C.; Hubbard, J. L. *Organometallics* **1996**, *15*, 1230.

dissociation having values ranging from 49 to 6.05 ($\times 10^{-4}$) s^{-1} at 0 °C. Furthermore, it was illustrated that the tungsten orotate derivative undergoes stereoselective CO exchange, with the CO ligands cis to the pseudoamido group being exchanged at a faster rate. These results clearly demonstrate that the unsaturated metal center, resulting from CO dissociation, is competitive with the pseudoaromatic uracil ring system for the electron density provided by the amido ligand. *Nevertheless, unlike the bis-amido* $(NH-C_6H_4-NH)^{2-}$ *or amidophenoxide* $(NH-C_6H_4-O)^{2-}$ *ligands which afford stable group 6 metal tricarbonyl species, there is no evidence other than kinetic data for the intermediary of a "16-electron" complex containing the orotate ligand.* As anticipated, upon hydrogenation of the orotate ring where it is no longer pseudoaromatic, the CO ligands in the $M(CO)_4$ unit are even more labile, indicative of the deprotonated nitrogen (1) atom being more amide-like in character. A similar CO-labilizing effect was seen in the $W(CO)_5$(uracilate)$^-$ derivative where the CO ligands are highly labile relative to saturated amine metal analogues.

Acknowledgment. The financial support of this research by the National Science Foundation (Grant CHE96-15866) and the Robert A. Welch Foundation is greatly appreciated.

Supporting Information Available: X-ray crystallographic files, in CIF format, for complexes **1**, **2**, and **4** are available on the Internet only. Access information is given on any current masthead page.

Note Added in Proof

Subsequent to the submission of this manuscript it has become apparent that zinc is indeed present in the OMP decarboxylase enzyme (Miller, B. G.; Traut, T. W.; Wolfenden, R. *J. Am. Chem. Soc.* **1998**, *120*, 2666).

IC980233F